Chapter 1

Self-Oscillatory DC-DC Converter Circuits for Energy Harvesting in Extreme Environments

Ming-Hung Weng, Daniel Brennan, Nick Wright and Alton Horsfall

Additional information is available at the end of the chapter

http://dx.doi.org/10.5772/intechopen.72718

Abstract

A novel self-starting converter circuit technology is described for energy harvesting and powering wireless sensor nodes, constructed from silicon carbide devices and proprietary high temperature passives for deployment in hostile environments. After a brief review of the advantages using Silicon Carbide (SiC) over other semiconductors in extreme environments, the chapter will describe the advantages and principles when designing circuitry and architectures using SiC for power electronics. The practical results from a novel self-starting DC-DC converter are reported, which is designed to supply power to a WSN for deployment in high temperature environments. The converter operates in the boundary between continuous and discontinuous mode of operation and has a Voltage Conversion Ratio (VCR) of 3 at 300°C. This topology is able to self-start and so requires no external control circuitry, making it ideal for energy harvesting applications, where the energy supply may be intermittent. Experimental results for the self-starting converter operating from room temperature up to 300°C are presented. The converter output voltage, switching frequency, total power loss and efficiency were presented at temperatures up to 300°C.

Keywords: wide band gap semiconductors, silicon carbide, SiC, energy harvesting, wireless sensor networks, high temperature circuit, switching frequency, MOSFETs, JFETs, DC-DC power converters, field effect transistor switches

1. Introduction

In recent years there has been increasing demand to investigate and monitor ever more hostile environments including those containing high temperatures and/or extreme radiation flux [1–3]. Silicon carbide (SiC) boasts a much higher band gap than conventional silicon and is therefore

more chemically stable allowing electronic circuits made from this material to be deployed in environments where conventional silicon based electronics cannot function.

The development of silicon carbide (SiC) technology has become increasingly rapid in recent years with significant improvements in wafer and epitaxy growth technology of 8-inch and beyond [4]. By offering scalable and cost-effectively materials processing, SiC devices have become part of the mainstream in power electronic applications [5, 6] and a number of conferences are running dedicated sessions to the deployment of this technology from niche to mainstream. Further advantages in terms of small, signal level devices [7], sensors [8] and CMOS circuitry [9] have resulted in significant improvements in capabilities, however these are still only available at research level, where a number of groups are active. During recent years, SiC has emerged as a promising material for electronics where the underlying rationale for the continued investment in SiC technology is the excellent material properties. SiC is the only technologically relevant semiconductor that has a stable thermal oxide (SiO_2) [10] and can exist in a large number of polytypes – different crystal structures built and derived from the high chemical stability of the SiC sub-unit organised into different stacking sequences. All forms of SiC are considered a wide bandgap material since the electronic bandgaps of the different polytypes range from 2.4 to 3.3 eV. The bandgap of 4H SiC is 3.23 eV at room temperature (compared to 1.12 eV for silicon) and this dramatically reduces the intrinsic carrier concentration in comparison to semiconductors such as silicon or gallium arsenide and this allows devices to theoretically operate at temperatures up to 1000°C [11]. Electrical properties of SiC tailored toward devices also has a high saturation electron velocity, 2×10^7 cm·s^{-1}, a thermal conductivity in excess of copper at room temperature and a critical electric field that is almost an order of magnitude higher than that of silicon. Fulfilling technical parameters and standards, SiC has been exploited in the high performance power MOSFETs and diodes that are commercially available, but also have the potential to realise high performance, high frequency oscillators, amplifiers and different topologies power inverters.

For these high temperature environments are incompatible with standard battery technologies, and so, energy harvesting is a suitable technology when remote monitoring of these extreme environments is performed through the use of wireless sensor nodes (WSNs) [12–14]. There is now a variety of energy harvesting devices available which are capable of producing sufficient energy from the ambient surroundings to intermittently power a WSN [15–17]. Energy harvesting devices often produce voltages which are unusable directly by electronic loads and so require power management circuits to convert the electrical output to a level which is usable by monitoring electronics and sensors. Therefore a DC-DC step-up converter that can handle low input voltages is required [18, 19]. The required gate-drive circuitry for these converters need to be placed next to the switches to minimise system complexity, however, the successful operation of the gate drivers, especially with no heat sink in hostile environments will increase the power density for DC-DC converter modules. The advantages of SiC based power devices include high current densities, faster switching speeds and high temperature capabilities. To fully utilise the benefits of SiC devices in DC-DC converters used in harsh environments, the gate drive design requires special attention. To match the high temperature capabilities of SiC devices, the gate drivers also need to be capable of operation at these elevated temperatures [20, 21].

SiC based switches such as SiC JFETs are capable of tolerating these elevated temperatures, however, various other components such as passives, magnetics or amplifiers will make this task rather challenging. From a system point of view, the gate drive requirements of normally-on SiC JFETs are a significant challenge. The issue with the start-up process in addition to the differences in the gate voltage requirements make them less desirable for power designers [22, 23]. However, the specific on-resistance of normally-off (enhancement-mode) JFETs is almost 15% higher than their normally-on counterparts [24]. Therefore in a circuit where on state losses are expected to be the dominant power losses, the normally-on (depletion mode) JFETs are better alternatives. Another disadvantage of normally-off SiC JFETs is that in order to keep the device in the on state, the gate-source junction must be forward biased [25]. This implies that similar to SiC based BJTs, there is a considerable drive current requirement, which undesirable.

2. Power sources and energy options for wireless sensor nodes

2.1. Power sources for wireless sensor nodes

Wireless sensor networks have become a very popular enabling technology and have already entered the market place in a number of sectors. The majority of these platforms are powered by limited-life batteries. Hence alternative power sources are being continuously investigated and employed [26].

The rapid reduction in the size and power consumption of electronic components has helped speed up the research on communication nodes and wireless sensors. As the size of these WSNs decreases, their use becomes more widespread in the automobile industry, industrial environments and aerospace industry. However, their respective power supply has become a major issue, because the size reduction in CMOS electronics has significantly outpaced the energy density improvements in batteries, which are the most commonly used power sources. Consequently, the power supply is the limiting factor on both the size and lifetime of the sensor node. Energy reservoir power sources such as micro-scale batteries, micro-fuel cells, ultra-capacitors are characterised by their energy density and can be used to power WSNs but at the cost of increased size and reduced lifetime. Power scavenging sources are an alternative power source. Unlike energy reservoirs, power scavenging sources are characterised by their power density; the energy provided from these sources depends on the amount of time each source is in operation [26–29]. One of the popular power scavenging sources is via temperature gradients [30, 31]. Energy can be scavenged from the environment using the temperature variations that naturally occur. The maximum power-conversion efficiency from a temperature difference, the Carnot efficiency is given below in Eq. (1), where the temperature is in Kelvin:

$$\eta = \frac{\left(T_{high} - T_{low}\right)}{T_{high}} \tag{1}$$

Assuming a room temperature of 27°C and for a source 5°C above room temperature, the maximum efficiency is 1.64% and for a source 10°C above room temperature is maximum efficiency is 3.22%. At low temperature differences and small scales, conduction will dominate

and convection and radiation can be neglected. The heat flow through conduction is given by Eq. (2), where L is the length of material that the heat is flowing through and k is the thermal conductivity of the material used:

$$q' = k\frac{(\Delta T)}{L} \tag{2}$$

Assuming a length of 1 cm and a temperature difference of 10°C, the heat flow (power) for silicon with a thermal conductivity of 140 W/mK is 14 W/cm^2. Assuming that Carnot efficiency could be achieved, the output power would be 451 mW/cm^2 which is significantly higher than comparable power sources. In practice, the efficiencies for this type of energy harvester are well below the Carnot efficiency. One of the most common ways to convert the generated power from temperature differences to electricity is by using thermoelectric generators.

2.2. Thermoelectric generators

Driving a wireless sensor node from ambient is attractive as it eliminates the need for wires or batteries. Despite the clear advantages of energy harvesting, these systems require a suitable power management strategy to convert the low voltage levels to a level usable by the wireless sensor systems. Many WSNs monitor physical quantities, which change slowly and therefore the measurements can be taken and transmitted less frequently. This means lower operating duty cycle and therefore many wireless sensor systems consume very low average power, hence they are suitable candidates for energy harvesting power sources.

Thermoelectric generators (TEGs) are energy harvesting devices capable of producing large amounts of current at low voltages from a thermal gradient across the device; through a phenomenon known as the Seebeck effect [32]. Modern TEG's are constructed out of p-n junctions of different semiconductor materials depending on their operational requirements, but commonly bismuth telluride (Bi_2Te_3). The mechanical construction of a typical TEG is shown in **Figure 1**.

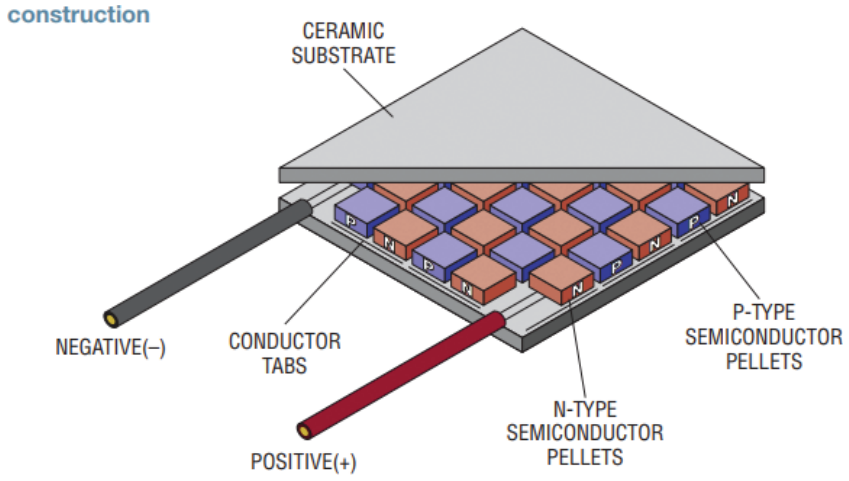

Figure 1. Construction of a thermoelectric generator [33].

In this work a standard off-the-shelf TEG manufactured by Marlow (product number TG 12-801 L) was characterised in terms of the electrical output as a function of temperature difference between the two surfaces. A ceramic hotplate was used to provide a controlled temperature heat source whilst a thermocouple embedded into the base of a heat sink and fan provided the cooler side thus creating a measurable temperature difference across the device. The higher the temperature difference, the greater the output voltage becomes at any given current. **Figure 2** shows the output power of the thermoelectric generator as a function of the output voltage. The solid line intersects with the waveforms where the maximum output power is at the optimum output voltages. The optimum voltage for the TEG is generally below 1.3 V and needs to be boosted in order to enable the operation of the circuit for remote sensor applications.

2.3. The need for a high temperature self-starting DC-DC converter

In addition to the Voltage Conversion Ratio (VCR) requirements to supply a SiC sensor circuit, operating in a very high temperature environment (up to 300°C) demands a high temperature step-up DC-DC converter. In addition to the power stage of the converter, the gate-drive circuitry is also required to operate at elevated temperatures. To eliminate the need for a high temperature gate driver and also to reduce the size of the power management circuitry, a self-starting DC-DC converter is desired [34]. Here, a self-starting DC-DC converter was designed to boost the low DC output voltage of a thermoelectric generator to a level sufficient to run a SiC sensor circuit for wireless monitoring of inhospitable environments [35–37]. These environments may be subject to high temperatures in the case of exhaust gas monitoring in turbine engines or oven environments, they may also be subject to radiation in the nuclear industry whether they are used in power generation or waste monitoring. The proposed DC-DC converter does not need an auxiliary power supply to drive the normally-on JFET. The converter self-starts and does not suffer from a start-up shoot through. The requirement of self-oscillation needs a depletion mode device (e.g. normally-on JFET) as there will be no current flowing at start otherwise.

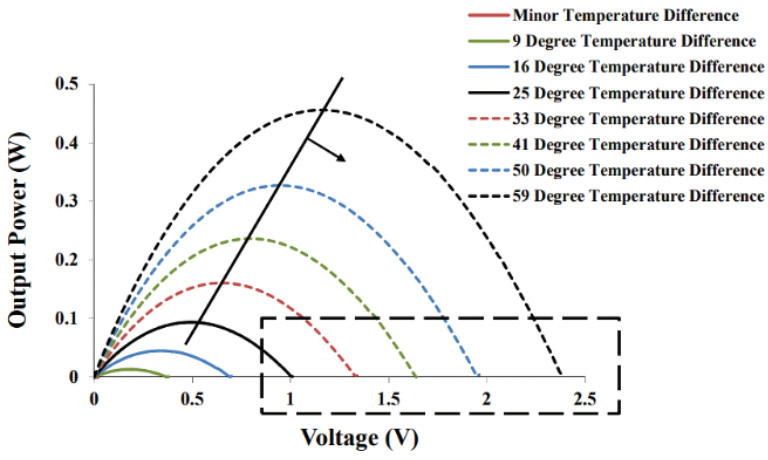

Figure 2. Output power as a function of voltage for the thermoelectric generator for various temperature differences.

3. Theory behind the self-starting DC-DC converter

Figure 3 shows the circuit diagram of the proposed self-starting DC-DC converter designed for boosting low level voltages from the TEG, denoted in the **Figure 3** as V_{in}. The input capacitance of the circuit, C_{in}, represents the capacitance of the p-n junctions of the TEG. Based upon a standard boost converter topology and a blocking oscillator, the key aspect of the design is the use of a counter-wound secondary winding in conjunction with a normally-on device which is used to provide the self-oscillatory behaviour, thus eliminating the need for an external gate drive [38]. The elimination of a separate gate drive is crucial for the successful commissioning of a silicon carbide energy harvesting system designed for use with low voltage DC sources such as solar cells and thermogenerators. The voltages provided by these sources are magnitudes smaller than the voltages required to provide the gate drive requirements for a conventional converter topology; therefore a self-oscillating design becomes the only viable option.

The simplicity of the design is also important when considering the capability of high temperature components. At present, commercially available SiC components are limited to discrete power devices and do not include the control circuitry required for complex designs. The commercial drive behind silicon carbide electronic devices to date has been focussed on the power electronics market, where the ability of silicon carbide to operate at high frequencies and with low power losses has been utilised for the realisation of highly efficient circuits that offer significant space saving over conventional systems. Here it is demonstrated that the ability of silicon carbide components to operate at these high temperatures can be harnessed for the production of a step-up converter with the ability to power circuits within the high temperature environment itself, with minimum component count, thus reducing the overall cost of a high temperature energy harvesting system.

3.1. Principle of operation

As shown in **Figure 4**, the self-oscillating converter circuit uses a depletion mode JFET and a Schottky diode in a boost configuration, wherein coupled inductors are used to feed the gate-source of the SiC based switching device and act to initialise the oscillations. The operation of the circuit is as follows; at start-up and as the input voltage rises, the SiC JFET as a normally-on device conducts and the current flows through the inductor. The current in the primary

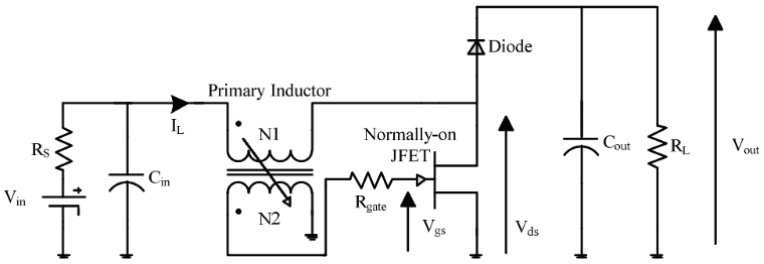

Figure 3. The proposed self-starting boost converter.

http://dx.doi.org/10.5772/intechopen.72718

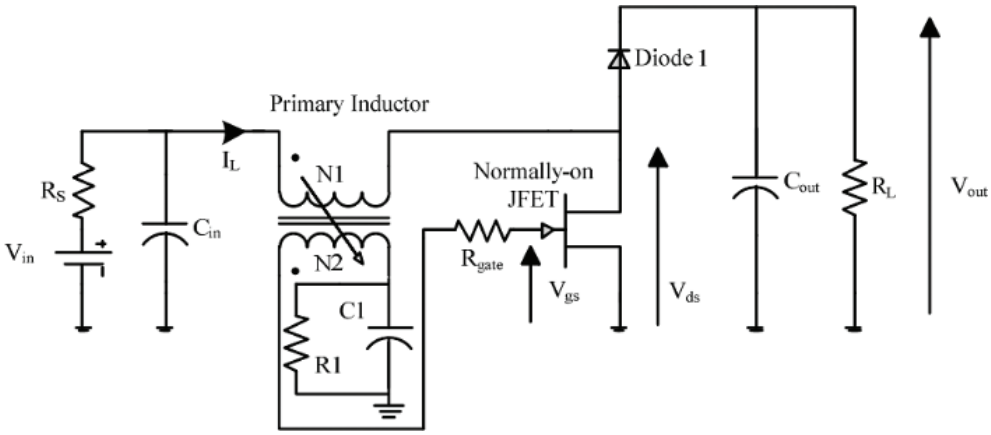

Figure 4. The self-starting step-up converter with the paralleled RC.

winding of the coupled inductor increases exponentially with time reducing the voltage across the primary winding, inducing a voltage on the secondary winding of the transformer due to the change in the primary current. Capacitor C1 is charged to a negative voltage with respect to the circuit ground. When the bias across the capacitor exceeds the pinch off potential of the JFET, the on state resistance of the JFET increases, so that the current through the FET drops to zero. This reduction in current flowing through the JFET results in the decrease in the current flow through the primary winding of the transformer. When the current in the primary winding becomes zero, the voltage on the secondary winding reaches zero as well and C1 is discharged through the resistor R1 to ground. Once the bias across the capacitor falls below the pinch off potential of the JFET, the on state resistance of the JFET reduces significantly, current flows through the primary winding of the inductor and the circuit operation repeats. The switching frequency of the converter is determined primarily by the gate-source capacitance of the SiC JFET and the inductance of the primary side of the drive transformer.

As shown by the circuit topology in **Figure 5** the RC circuit connected to the JFET gate can be removed and the secondary winding directly connected to ground. The stray capacitance of the primary winding is sufficient to enable the self-oscillation occur and the converter operates without the inclusion of the external RC components.

When the normally-on silicon carbide JFET conducts, current begins to flow through the primary winding of the transformer and the channel of the JFET to ground, this induces a negative bias in the secondary winding. As the current flowing through the primary winding increases, the negative voltage on the secondary winding increases in magnitude and the channel of the JFET is progressively pushed toward pinch off. Once the magnitude of the voltage on the secondary winding reaches the threshold voltage of the JFET, the JFET becomes non-conducting. This causes the magnetic field contained in the ferrite core of the transformer to collapse and the voltage in the primary winding increases as is observed in a standard boost converter topology. Whilst the JFET is non-conducting, power is transferred to the output

through the silicon carbide Schottky diode at a higher voltage level. The voltage induced on the secondary winding then drops due to reduced current flow in the primary and the JFET transistor becomes conducting again to complete the switching cycle.

During operation the converter operates at the boundary between Continuous Conduction Mode (CCM) and Discontinuous Conduction Mode (DCM), the operating point often described as critical conduction mode. When the JFET is non-conducting, the voltage induced on the secondary winding decreases due to reduced current flow in the primary. Therefore the JFET becomes fully conducting again when the inductor current has reached zero, which results in a zero voltage on the gate of the normally-on JFET. The schematic in **Figure 6** illustrates the current waveform in the primary inductor for a converter operating in critical conduction mode. During the on time (denoted by DT) the energy stored in the inductor increases and during the off-state (the remainder of the waveform) the inductor fully discharges. The end of the switching period coincides with the point at which the current through the inductor and hence the energy stored in the inductor falls to zero. In **Figure 6**, the average current I_{avg} is half the peak current, I_{peak}. This peak current is determined by the rate of change of current through the primary inductor during the charging and discharging portions of the waveform.

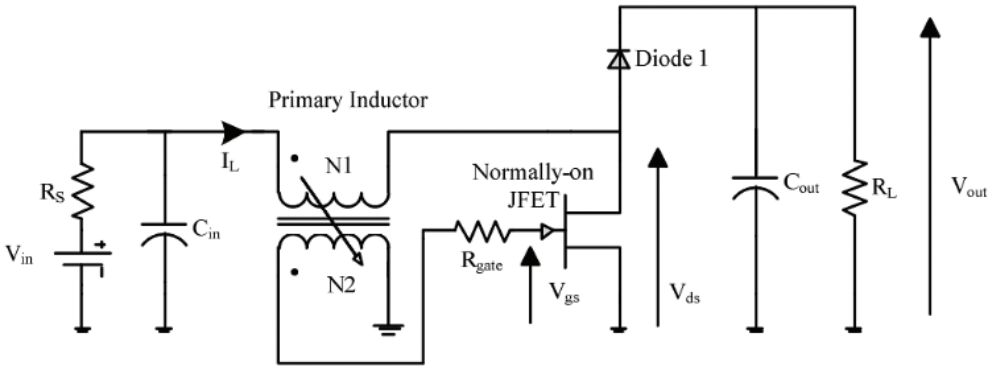

Figure 5. The self-starting step-up converter without the paralleled RC.

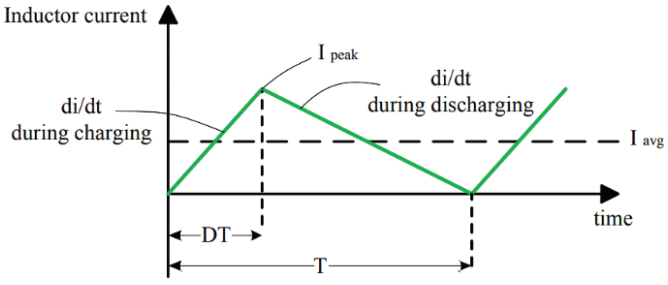

Figure 6. The critical mode of operation, boundary between CCM and DCM.

4. The self-starting DC-DC converter

4.1. Experimental results

The SiC JFET and SiC Schottky diode were packaged in high temperature ceramic packages and the circuit was tested in a temperature controlled oven. Both the Schottky diode and JFET were fabricated using process techniques developed at Newcastle University [39–41]. The data in **Figure 7** show the I-V characteristics of the JFET used in the circuit.

Of note is the pinch off potential of the device, which is approximately −6.5 V, which is found to be optimal. FETs with a more negative pinch potential require a higher rate of change of current through the primary inductor in order to pinch off the channel – making them unsuitable for use in energy harvesting environments. A pinch off potential closer to zero offers advantages in terms of requiring a lower rate of change of current through the primary inductor. However, when the gate voltage is zero, the on state resistance of the channel is higher [42] and this reduces the efficiency of the converter. As shown by the circuit schematic in **Figure 8**, a 100 kΩ resistor was used as the load to mimic a wireless sensor node designed for high temperature energy harvesting applications. Typically due to the low power levels available in a circuit powered by energy scavenging, sensor nodes are designed to intermittently use the power generated, thus reducing the time averaged power draw, as there is insufficient power generated to continuously run a sensor node. This is specifically relevant where the node is based on the wireless transmission of data to a remote access node [43].

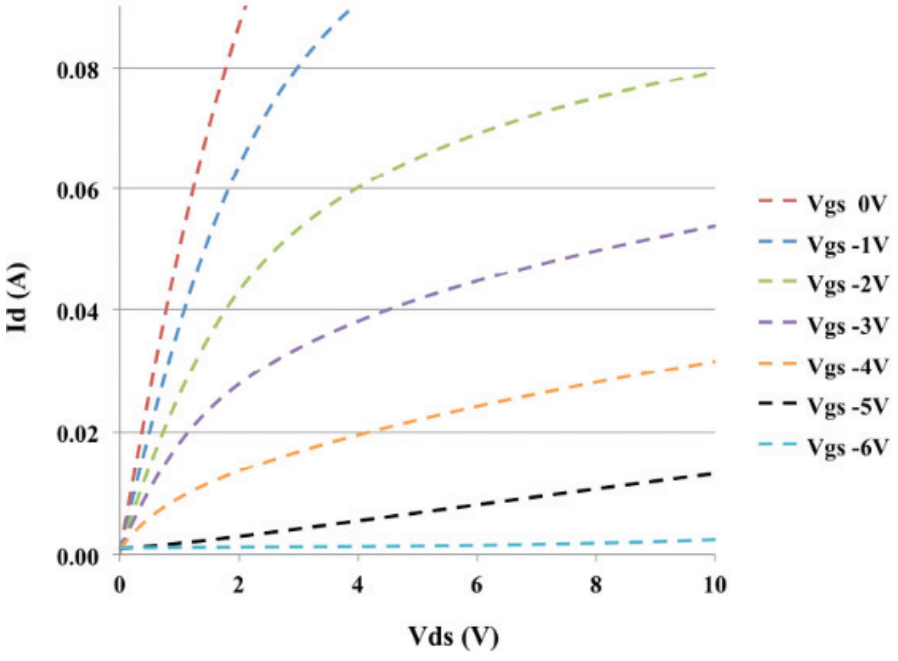

Figure 7. I-V characteristics of the SiC JFET used in the converter at 25°C.

The data in **Figure 9** show the voltage waveforms of the JFET during room temperature operation with an input voltage of 1 V. From **Figure 9** it can be observed that the gate voltage of the FET (denoted by Vgs) reaches the pinch off potential, setting the current thorough the FET to zero, before rapidly becoming positive, resulting in a significant reduction in the on state resistance. The voltage across the FET channel, denoted by Vds, increases as the gate voltage becomes more negative, reaching a value of 5.5 V when the channel is fully pinched off. This enhancement in the voltage across the FET in comparison to the input voltage arises from the energy stored in the inductor and is the fundamental principle behind the operation of a boost converter. The voltage across the JFET reduces to zero when the gate voltage is positive, showing that the JEFT is conducting.

The data in **Figure 10** show the variation in converter output voltage as a function of temperature for a range of input voltages that are relevant to energy harvesting from a thermoelectric generator. It can be seen that the boost converter can successfully operate at input voltages

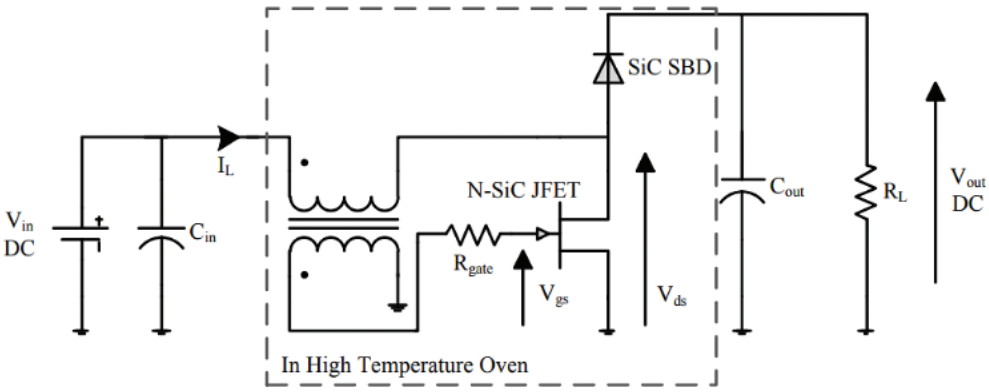

Figure 8. Schematic of the SiC self-starting DC-DC converter.

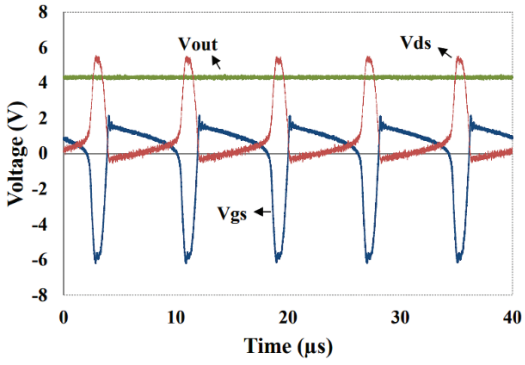

Figure 9. Voltage waveforms of the self-starting boost converter.

between 1.3 and 2.5 V over the full 300°C range, demonstrating boost capabilities of up to 4.5 times the input voltage. At higher temperatures, the output voltage drops due to the increased SiC diode forward voltage drop, increased JFET on-resistance and increased copper loss in the inductor windings. The effect of these is also apparent in the data shown in **Figure 12**. At input voltages below 1.2 V, the converter does not self-start at high temperatures. At input voltages of 1, 1.1 and 1.2 V the converter failed to self-start at temperatures above 150, 200 and 250°C, respectively. This is thought to be related to the reduction of the mutual inductance between the primary and secondary windings of the inductor caused by the magnetic properties of the ferrite being adversely affected. Therefore the voltage induced in the secondary as a result of the rate of change of current in the primary winding is lower, resulting in the gate voltage of the JFET being insufficient to reach the pinch off potential. In this situation the current through the JFET does not reduce to zero and the energy stored in the inductor is not transferred to the load as the voltage is lower than the turn on voltage of the diode and the converter does not operate.

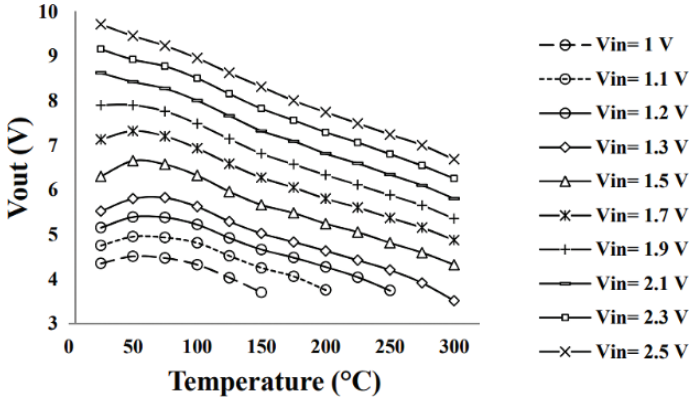

Figure 10. Output voltage as a function of temperature.

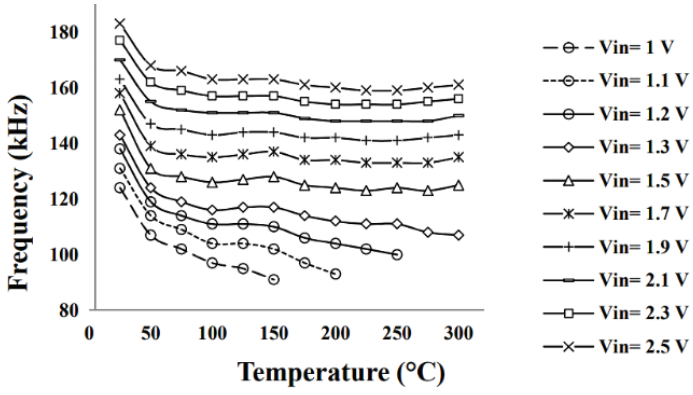

Figure 11. Switching frequency as a function of temperature.

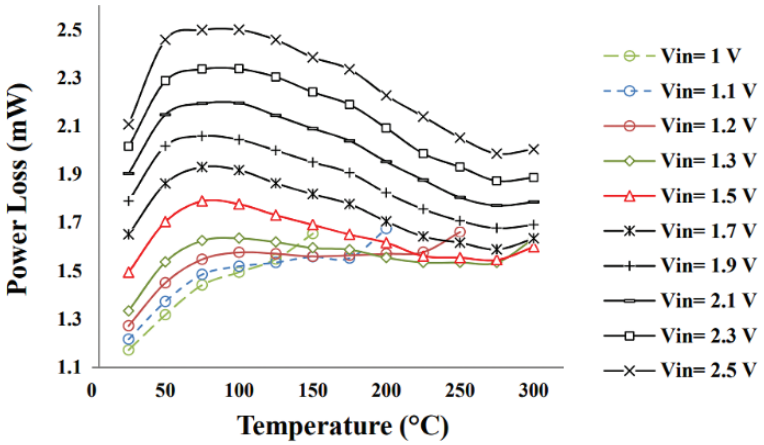

Figure 12. Power losses as a function of temperature.

In order to enable operation at lower input voltages, the turns ratio between the primary and secondary coils of the transformer can be increased, however this is limited by the physical size of the ferrite core used in this work. Based on the data shown in **Figure 8**, it can be seen that this converter is capable of boosting the energy harvested from a thermogenerator with a temperature difference of 40°C. Energy harvesting from lower temperature differences is possible using two thermogenerators connected electrically in series but thermally in parallel.

The results in **Figure 11** show the effect of temperature on the operating frequency of the circuit. As described previously, the frequency of operation is determined by the rate of change of current in the primary winding of the transformer (which can be described in terms of the inductance of the winding) and the input voltage from the thermogenerator. This is directly related to change in the material properties of the ferrite core with temperature. As the temperature increases, the permeability and saturation magnetisation of the ferrite core reduces, resulting in the shift in the magnitude of the inductance of the primary winding. Therefore increasing the ambient temperature from 25 to 300°C, results in the switching frequency of the converter decreasing from 183 to 161 kHz and from 143 to 107 kHz at input voltages of 2.5 and 1.3 V, respectively. As can be seen from the data in **Figure 11**, the switching frequency also increases with input voltage when increasing the supply from 1 to 2.5 V. This increase is directly linked to the rate of change of current in the primary winding.

The overall power losses and efficiency of the converter circuit as a function of temperature is shown in **Figures 12** and **13**, respectively. As can be seen from the data, the efficiency is lower at higher temperatures. This reduction is to be expected, as the resistance of the JFET channel increases due to the reduction in electron mobility [44] and the parasitic resistance of the inductor winding increasing. The diode voltage drop of the SiC Schottky diode also increases with temperature [45], however the effect is minor in comparison to the changes in the JFET and inductor. Hence, the overall power losses in the circuit increase. Increasing the input voltage results in higher power losses in the converter, due to the increased reverse voltage

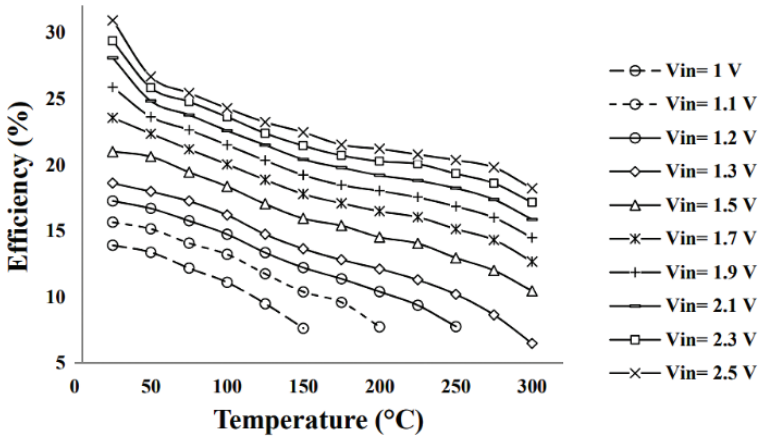

Figure 13. Efficiency of boost converter as a function of temperature.

across the SiC JFET during switching. The current ripple in the inductor also increases, resulting in higher conduction losses in the inductor. As the output voltage changes with temperature, the output power transferred to the constant resistive load also changes with temperature.

As can be seen from the data in **Figure 12**, the increasing temperature results a reduction in the overall power losses; which can be explained by the reduced current in the resistive load due to the reduced output voltage. The reduction in the output voltage with temperature results in a reduced drain-source voltage for the JFET, resulting in the JFET operating in the linear region (as can be seen from the data in **Figure 7**), resulting in the SiC JFET acting more like a resistor at temperatures above 275°C and so the power losses start to increase with temperature. This can be seen in **Figure 12** for the data relating to input voltages of 1 and 1.1 V, where a significant increase in power loss occurs at 150 and 200°C respectively. As the output power from the converter is low, the losses in the circuit will play a significant role in the overall efficiency of the circuit.

To assess the converter performance at higher output currents, a 10 kΩ resistor was connected as the load and the converter performance was characterised for a range of input voltages at different temperatures. The converter output voltage as a function of temperature for a range of input voltages is shown by the data in **Figure 14**. As can be seen from the data, the output voltage of the converter decreases as the temperature increases, in a manner similar to that for the 100 kΩ load, as shown in **Figure 10**. At higher output current levels, the overall conduction and switching losses increase in the converter, resulting in a drop of the output voltage. As the load current has increased (10 kΩ), the output voltage of the converter is lower when compared to the case with a 100 kΩ load, due to the increased conduction losses.

Similarly to the operation of the converter with the 100 kΩ output resistor, at input voltages below 1.3 V, the converter is not capable of self-starting at high temperatures. At input voltages of 1, 1.1, 1.2 and 1.3 V the converter did not self-start at temperatures above 125, 175, 200 and 250°C,

respectively. At a higher output current, the effective voltage across the primary inductor is lower; due to the increased voltage drop across the parasitic resistance in the inductor, resulting in a lower induced voltage in the secondary winding. As described for the 100 kΩ load above, if this gate voltage on the JFET, which is equal to the voltage induced in the secondary winding does not reach the pinch off potential of the device, the converter will not oscillate. Hence for the higher output current (10 kΩ load) the converter is capable of self-starting operation at lower temperatures in comparison to the case with a 100 kΩ load resistor.

The converter overall efficiency as a function of temperature is shown by the data in **Figure 15**. As can be seen from the data, the efficiency of the converter is approximately twice that of the

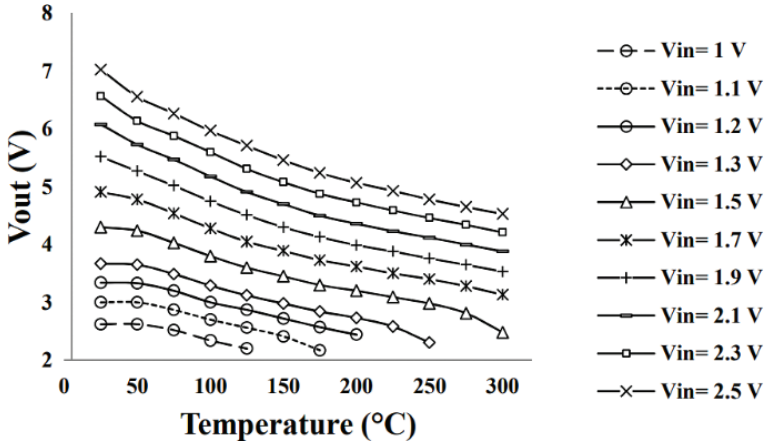

Figure 14. Output voltage as a function of temperature.

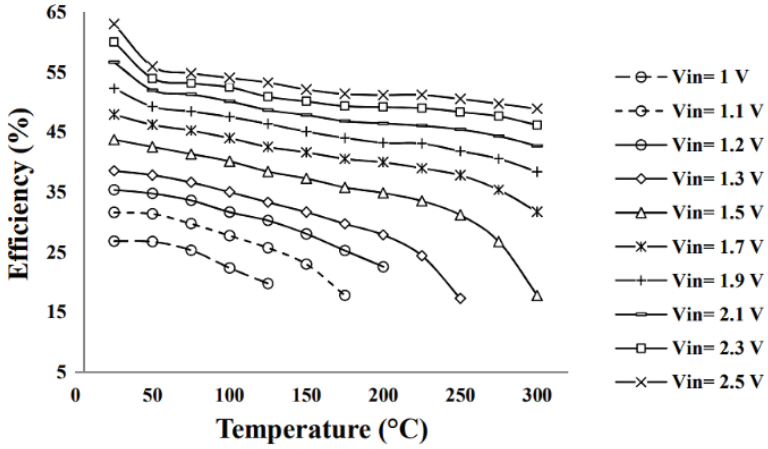

Figure 15. Efficiency of boost converter as a function of temperature.

converter supplying a 100 kΩ load. As described for the 100 kΩ converter, at higher temperatures the increased resistance of both the JFET channel and the windings within the transformer itself result in a reduction in efficiency. The SiC diode voltage drop also increases with temperature, so the overall conduction loss in the circuit increases, resulting in a decrease in the system efficiency. However, it can be seen from the data that the decrease in efficiency with increasing temperature is not as significant for the high output power circuit. As the converter output power is significantly higher, the power losses in the circuit will play a less significant role in the overall efficiency of the converter hence the converter efficiency is higher.

5. Conclusions

A novel self-starting converter technology has been described, which is suitable for powering wireless sensor nodes by means of energy harvesting from a thermal gradient. The converter was constructed from silicon carbide devices and proprietary high temperature passives to enable deployment in hostile environments, such as those found in aerospace, oil and gas and nuclear applications. The self-oscillating nature of the circuit along with high temperature capability result in reduced component count and hence a more reliable approach for powering SiC based WSNs for hostile environments. The self-oscillating nature of the circuit along with high temperature capability result in reduced component count and hence a more reliable approach for powering SiC based WSNs for hostile environments. The operation principle of the self-starting converter was detailed for two configurations which reflect low and high output current. The effect of input voltage and primary inductance on the converter operation and switching frequency was correlated with the characteristics of the components used in the circuit manufacture and the operating conditions for the circuit. Experimental measurements on a converter showed that whilst the performance of the circuit is influenced by the ambient temperature, it is possible to boost the voltage from a thermoelectric generator to a level that is suitable for the operation of high temperature circuits.

Author details

Ming-Hung Weng[1], Daniel Brennan[1,2], Nick Wright[1] and Alton Horsfall[1]*

*Address all correspondence to: alton.horsfall@ncl.ac.uk

1 School of Engineering, Newcastle University, Newcastle upon Tyne, UK

2 IsoCom Limited, Washington, UK

References

[1] Issa F et al. Radiation silicon carbide detectors based on ion implantation of boron. IEEE Transactions on Nuclear Science. 2014;**61**:2105-2111

[2] Hornberger J, et al. Silicon-carbide (SiC) semiconductor power electronics for extreme high-temperature environments. In: 2004 IEEE Aerospace Conference Proceedings; 2004. pp. 2538-2555

[3] Lees JE et al. SiC X-ray detectors for harsh environments. Journal of Instrumentation. 2011; **6**:C01032

[4] Global Power SiC Epitaxial Wafer Mission Statement [Internet]. Available from: http://www.gptechgroup.com/pdf/Epitaxy.pdf

[5] Silicon Carbide Power Semiconductors [Internet]. Available from: www.littelfuse.com/products/power-semiconductors/silicon-carbide.aspx

[6] SiC and GaN Power and RF Solutions [Internet]. Available from: www.wolfspeed.com

[7] Chan HK et al. Silicon carbide based instrumentation amplifiers for extreme applications. In: 2015 IEEE Sensors conference; 2015. pp. 1-4

[8] Weng MH et al. Trap-assisted gas sensing mechanism in $Pd/TiO_2/SiO_2/SiC$ capacitors at high temperatures. IEEE Sensors Journal. 2007;**7**(10):1395-1399

[9] Weng MH et al. Recent advance in high manufacturing readiness level and high temperature CMOS mixed-signal integrated circuits on silicon carbide. Semiconductor Science and Technology. 2017;**32**:054003

[10] Cooper JA et al. Status and prospects for SiC power MOSFETs. IEEE Transactions on Electron Devices. 2002;**49**(4):658-664

[11] Zetterling CM. Process Technology for Silicon Carbide Devices. London: Inspec Publishing; 2002. ISBN 0852969988

[12] Nambiar SG, Ranjan P. Energy harvesting system for deployment of Wireless Sensor Networks in Nuclear Fusion Reactor. In: 2012 International Conference on Green Technologies (ICGT); 2012. pp. 288-292

[13] Lu X, Yang SH. Thermal energy harvesting for WSNs. In: 2010 IEEE International Conference on Systems Man and Cybernetics (SMC); 2010. pp. 3045-3052

[14] Zhang SS et al. LiBOB-based gel electrolyte Li-ion battery for high temperature operation. Journal of Power Sources. 2006;**154**:276-280

[15] Cid-Fuentes RG et al. Energy buffer dimensioning through energy-Erlangs in Spatio-temporal-correlated energy-harvesting-enabled wireless sensor networks. IEEE Journal on Emerging and Selected Topics in Circuits and Systems. 2014;**4**:301-312

[16] Li Y et al. Energy-prediction scheduler for reconfigurable systems in energy-harvesting environment. IET Wireless Sensor Systems. 2014;**4**:80-85

[17] Azevedo JAR, Santos FES. Energy harvesting from wind and water for autonomous wireless sensor nodes. IET Circuits, Devices and Systems. 2012;**6**:413-420

[18] Kim J, Kim C, DC-DC Boost A. Converter with variation-tolerant MPPT technique and efficient ZCS circuit for thermoelectric energy harvesting applications. IEEE Transactions on Power Electronics. 2013;**28**:3827-3833

[19] Cao X et al. Electromagnetic energy harvesting circuit with feedforward and feedback DC-DC PWM boost converter for vibration power generator system. IEEE Transactions on Power Electronics. 2007;**22**:679-685

[20] Valle-Mayorga J et al. High-temperature silicon-on-insulator gate driver for SiC-FET power modules. IEEE Transactions on Power Electronics. 2012;**27**:4417-4424

[21] Huque MA et al. A 200 °C universal gate driver integrated circuit for extreme environment applications. IEEE Transactions on Power Electronics. 2012;**27**:4153-4162

[22] Mino K et al. A gate drive circuit for silicon carbide JFET. In: The 29th Annual Conference of the IEEE Industrial Electronics Society, 2003. IECON '03; 2003. pp. 1162-1166

[23] Round S et al. A SiC JFET driver for a 5 kW, 150 kHz three-phase PWM converter. In: Conference Record of the 2005 Industry Applications Conference, 2005. Fourtieth IAS Annual Meeting; 2005. pp. 410-416

[24] Casady JB et al. A comparison of 1200 V normally-off & normally-on vertical trench SiC power JFET devices. Materials Science Forum. 2010;**679-680**:641-644

[25] Norling K et al. An optimized driver for SiC JFET-based switches enabling converter operation with more than 99% efficiency. IEEE Journal of Solid-State Circuits. 2012;**47**: 3095-3104

[26] Dilhac JM, Bafleur M. Energy harvesting in aeronautics for battery-free wireless sensor networks. IEEE Aerospace and Electronic Systems Magazine. 2014;**29**:18-22

[27] Paradiso JA, Starner T. Energy scavenging for mobile and wireless electronics. IEEE Pervasive Computing. 2005;**4**:18-27

[28] Vyas R et al. Inkjet printed, self powered, wireless sensors for environmental, gas, and authentication-based sensing. IEEE Sensors Journal. 2011;**11**:3139-3152

[29] Li Y et al. Hybrid micropower source for wireless sensor network. IEEE Sensors Journal. 2008;**8**:678-681

[30] Carmo JP et al. Thermoelectric microconverter for energy harvesting systems. IEEE Transactions on Industrial Electronics. 2010;**57**:861-867

[31] Dalola S et al. Autonomous sensor system with power harvesting for telemetric temperature measurements of pipes. IEEE Transactions on Instrumentation and Measurement. 2009;**58**:1471-1478

[32] Prijic A et al. Thermal energy harvesting wireless sensor node in aluminum Core PCB technology. IEEE Sensors Journal. 2015;**15**:337-345

[33] Salerno D. Ultralow voltage energy harvester uses thermoelectric generator for battery-free wireless sensors. LT Journal of Analog Innovation. 2010;**20**(3):1-11

[34] Brennan DR, et al. Novel SiC self starting DC-DC converter for high temperature wireless sensor nodes. In: 2012 IEEE Sensors conference; 2012. pp. 1-4

[35] Bhatnagar P et al. Optimisation of a 4H-SiC enhancement mode power JFET for high temperature operation. Solid State Electronics. 2005;**49**(3):453-458

[36] Patil AC et al. Characterization of Silicon Carbide Differential Amplifiers at High Temperature. In: 2007 IEEE Compound Semiconductor Integrated Circuit Symposium (CSICS); 2007. pp. 1-4

[37] Wright NG, Horsfall AB. SiC sensors: A review. Journal of Physics D. 2007;**40**:6345-6354

[38] Leenarts D et al. Circuit design for RF transceivers. Boston: Kluwer; 2001; ISBN 978030 6479786

[39] Morrison DJ et al. Effect of post-implantation anneal on the electrical characteristics of Ni 4H-SiC Schottky barrier diodes terminated using self-aligned argon ion implantation. Solid State Electronics. 2000;**44**(11):1879-1885

[40] Nikitina IP et al. Structural pattern formation in titanium–nickel contacts on silicon carbide following high-temperature annealing. Semiconductor Science and Technology. 2006;**21**(7):898-905

[41] Mahapatra R et al. Effects of interface engineering for HfO_2 gate dielectric stack on 4H-SiC. Journal of Applied Physics. 2007;**102**(2):024105

[42] Mostaghimi O et al. Design and performance evaluation of SiC based DC-DC converters for PV applications. In: 2012 IEEE Energy Conversion Congress and Exposition (ECCE); 2012. pp. 3956-3963

[43] Yang G et al. Wireless compressive sensing for energy harvesting sensor nodes. IEEE Transactions on Signal Processing. 2013;**61**(18):4491-4505

[44] Neudeck PG et al. Assessment of durable SiC JFET technology for +600 °C to −125 °C integrated circuit operation. ECS Transactions. 2011;**41**(8):163-176

[45] Barker S, et al. High temperature vibration energy harvester system. In: 2010 IEEE Sensors conference; 2010. pp. 300-303